Journal of Hazardous Materials 190 (2011) 501–507

Contents lists available at ScienceDirect

Journal of Hazardous Materials

journal homepage: www.elsevier.com/locate/jhazmat

Removal of phosphate from aqueous solution by biochar derived from anaerobically digested sugar beet tailings

Ying Yao[a], Bin Gao[a,*], Mandu Inyang[a], Andrew R. Zimmerman[b], Xinde Cao[c], Pratap Pullammanappallil[a], Liuyan Yang[d,a]

[a] Department of Agricultural and Biological Engineering, University of Florida, Gainesville, FL 32611, United States
[b] Department of Geological Sciences, University of Florida, Gainesville, FL 32611, United States
[c] School of Environmental Science and Engineering, Shanghai Jiao Tong University, Shanghai 200240, China
[d] School of the Environment, Nanjing University, Nanjing 210046, China

ARTICLE INFO

Article history:
Received 31 January 2011
Received in revised form 17 March 2011
Accepted 21 March 2011
Available online 29 March 2011

Keywords:
Biochar
Phosphate
Adsorption mechanisms
Model

ABSTRACT

Biochar converted from agricultural residues or other carbon-rich wastes may provide new methods and materials for environmental management, particularly with respect to carbon sequestration and contaminant remediation. In this study, laboratory experiments were conducted to investigate the removal of phosphate from aqueous solution by biochar derived from anaerobically digested sugar beet tailings (DSTC). Batch adsorption kinetic and equilibrium isotherm experiments and post-adsorption characterizations using SEM–EDS, XRD, and FTIR suggested that colloidal and nano-sized MgO (periclase) particles on the biochar surface were the main adsorption sites for aqueous phosphate. Batch adsorption experiments also showed that both initial solution pH and coexisting anions could affect the adsorption of phosphate onto the DSTC biochar. Of the mathematical models used to describe the adsorption kinetics of phosphate removal by the biochar, the Ritchie *N*-th-order ($N = 1.14$) model showed the best fit. Two heterogeneous isotherm models (Freundlich and Langmuir–Freundlich) fitted the experimental isotherm of phosphate adsorption onto the biochar better than the Langmuir adsorption model. Our results suggest that biochar converted from anaerobically digested sugar beet tailings is a promising alternative adsorbent, which can be used to reclaim phosphate from water or reduce phosphate leaching from fertilized soils. In addition, there is no need to regenerate the exhausted biochar because the phosphate-laden biochar contains abundance of valuable nutrients, which may be used as a slow-release fertilizer to enhance soil fertility and to sequester carbon.

© 2011 Elsevier B.V. All rights reserved.

1. Introduction

The release of phosphate from both point and non-point sources into runoff may impose a great threat on environmental health [1] [2]. As a growth limiting nutrient, high level phosphate can promote excessive production of photosynthetic aquatic microorganisms in natural water bodies and ultimately becomes a major factor in the eutrophication of many freshwater and estuary coast ecosystems [3]. It is therefore very important to develop effective technologies to remove phosphate from aqueous solutions prior to their discharge into runoff and natural water bodies [4].

Many phosphate removal technologies including biological, chemical, and physical treatment methods have been developed for various applications, particularly for the removal of phosphate from municipal and industrial effluents [3]. Both chemical and biological treatments have been well documented and proven to be effective to remove phosphate from wastewater. Addition of chemicals, such as calcium, aluminum, and iron salts into wastewater is considered a simple phosphate removal technique, which separates the phosphate from aqueous system through precipitation [5–8]. However, the chemical precipitation methods require strict control of operating conditions and may potentially introduce new contaminants into the water such as chloride and sulfate ions [2,5,9]. Biological treatment of phosphate in waste effluents may have certain advantages over the chemical precipitation method because it does not require chemical additions and enhanced biological treatment has been reported to remove up to 97% of the total phosphorus in waste water [10]. This technology, however, is very sensitive to the operation conditions and its phosphate removal efficiency may be, at times, much less [11]. Both the chemical and biological treatment methods are also subjected to the costs and risks associated with phosphate-rich sludge handling and disposal [12].

Various physical methods have also been developed to remove phosphate from aqueous solution such as electrodialysis, reverse

* Corresponding author. Tel.: +1 352 392 1864x285; fax: +1 352 392 4092.
E-mail address: bg55@ufl.edu (B. Gao).

0304-3894/$ – see front matter © 2011 Elsevier B.V. All rights reserved.
doi:10.1016/j.jhazmat.2011.03.083

osmosis, and ion exchange [5,13,14]. However, most of these physical methods have proven to be either too expensive or inefficient. Simple physical adsorption might be comparatively more useful and cost-effective for phosphate removal. Several studies investigated activated carbons as phosphate adsorbents, but showed that the adsorption capacity was very low [1,15,16]. For example, Namasivayam and Sangeetha [16] reported that activated carbon made from coir pith with $ZnCl_2$-activation had a phosphate adsorption capacity of only 5100 mg kg^{-1}. Lower-cost materials, such as slag, fly ash, dolomite, and oxide tailings have also been explored by several studies as alternative adsorbents of phosphate from waste water [17–20].

Biochar is a low-cost adsorbent that is receiving increased attention recently because it has many potential environmental applications and benefits. While most of the current biochar studies are focused on biochar land application as an easy and cost-effective way to sequestrate carbon and increase fertility, a number of recent investigations suggest that biochar converted from agricultural residues have a strong ability to bind chemical contaminants in water including heavy metals and organic contaminants [21–25]. The use of biochar to remove phosphate from wastewater, however, is still a relatively less explored, though promising concept. Not only may biochar represent a low-cost waste water treatment technology for phosphate removal, but the phosphate-laden biochar may be used as a slow-release fertilizer to enhance soil fertility that will also sequester carbon. But little research has been conducted to explore the phosphate removal potential of biochar [26,27].

Yao et al. [27] characterized the physicochemical properties of two biochars and compared their phosphate removal abilities with activated carbon and their Fe-impregnated forms. The results showed that biochar derived from the residues of anaerobically digested sugar beet tailings had much better phosphate removal ability than all the other tested adsorbents. As a follow-up, laboratory adsorption experiments and mathematical models were used in this study to determine the mechanisms and characteristics of phosphate adsorption onto the digested sugar beet tailing biochar (DSTC). The specific objectives were to: (a) identify the mechanisms governing the adsorption of phosphate onto the DSTC; (b) measure the kinetics and equilibrium isotherms of phosphate adsorption onto DSTC; and (c) determine the effect of initial solution pH and coexisting anions on the adsorption of phosphate onto the DSTC.

2. Materials and methods

2.1. Materials

The biochar sample (DSTC) used in this study was obtained by pyrolyzing residues of anaerobically digested sugar beet tailings at 600 °C inside a furnace (Olympic 1823HE) in a N_2 environment for 2 h. The DSTC was then crushed and sieved to give a 0.5–1 mm size fraction. After washing with deionized (DI) water to remove impurities, the biochar samples were oven dried (80 °C) and sealed in container before use. Detailed information about biochar production and its physiochemical properties can be found in Yao et al. [27].

Phosphate solutions were prepared by dissolving potassium phosphate dibasic anhydrous (K_2HPO_4) in DI water. All the chemicals used in the study are A.C.S. certified and from Fisher Scientific.

2.2. Adsorption kinetics

Adsorption kinetics of phosphate onto DSTC were examined by mixing 0.1 g of the biochar with 50 mL phosphate solutions of 61.5 mg L^{-1} (20 mg L^{-1} Phosphorus) in 68 mL digestion vessels (Environmental Express) at room temperature (22 ± 0.5 °C). The pH was then adjusted to close to 7 prior to the measurements of the adsorption kinetics. The vessels were then shaken at 200 rpm in a mechanical shaker. At appropriate time intervals, the vessels were withdrawn and the mixtures were immediately filtered through 0.22 μm pore size nylon membrane filters (GE cellulose nylon membrane). The phosphate concentrations in the liquid phase samples were determined by the ascorbic acid method (ESS Method 310.1 [28]) and a spectrophotometer (Thermo Scientific EVO 60). Phosphate concentrations on the solid phase were calculated based on the initial and final aqueous concentrations. All the experimental treatments were performed in duplicate and the average values are reported. Additional analyses were conducted whenever two measurements showed a difference larger than 5%.

2.3. Adsorption isotherm

Adsorption isotherm of phosphate onto DSTC was determined similarly by mixing 0.1 g DSTC with 50 mL phosphate solutions of different concentrations ranging from 15 to 640 mg L^{-1} in the digestion vessels. After pH adjustment to about 7, the vessels were shaken in the mechanical shaker for 24 h at room temperature, this time period having been previously determined by kinetic experiments as sufficient for adsorption equilibrium to be established. The samples were then withdrawn and filtered to determine adsorbed phosphate concentrations by the same method. Following the experiments, the post-adsorption DSTC samples were collected, rinsed with DI water, and dried at 80 °C in an oven for further characterizations.

2.4. Effect of pH and coexisting anions

The effect of initial solution pH on phosphate removal was studied over a range of 2–11 (i.e., 2.0, 4.0, 6.2, 7.1, 8.1, and 10.4). In addition, the effect of the common coexisting anions, chloride, nitrate, and bicarbonate, was also investigated by adding 0.01 M of NaCl, $NaNO_3$, or $NaHCO_3$ to the 61.5 mg L^{-1} phosphate solutions into separate digestion vessels. The adsorbent to initial solution phosphate concentration was the same as the kinetics experiment. The vessels were shaken in the mechanical shaker for 24 h at room temperature. The same procedures were then used to determine aqueous and adsorbed phosphate concentrations.

2.5. Post-adsorption biochar characterization

To investigate the crystallographic structures on the post-adsorption DSTC, X-ray diffraction (XRD) patterns were acquired with a computer-controlled X-ray diffractometer (Philips APD 3720) equipped with a stepping motor and graphite crystal monochromator. Fourier transform infrared (FTIR) spectra were collected using a Bruker Vector 22 FTIR spectrometer (OPUS 2.0 software) to identify the surface functional groups of post-adsorption DSTC samples. The P-loaded DSTC was ground and mixed with KBr to approximately 0.1 wt% and pressed into a pellet using a mechanical device. Scanning electron microscopy (SEM, JEOL JSM-6400) coupled with dispersive X-ray spectroscopy (EDS, Oxford Instruments Link ISIS) was used to examine the surface of the post-adsorption DSTC and to determine its surfacial elemental composition. These characteristics of the phosphate-loaded DSTC were compared with those of the original biochar [27] to determine the adsorption mechanisms.

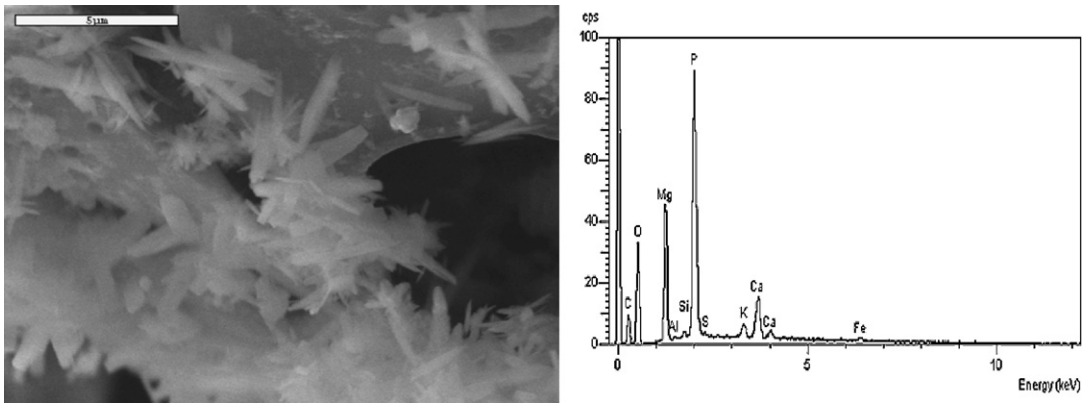

Fig. 1. SEM image (left) and corresponding EDS spectra (right) of the post-adsorption DSTC at 7000×. The EDS spectra were recorded at the same location as showing in the SEM image.

3. Results and discussion

3.1. Main adsorption mechanism

Surface characterization [27] showed that DSTC had a relatively high surface area measured with N_2 (336 $m^2\,g^{-1}$) and CO_2 (449 $m^2\,g^{-1}$), which is generally desirable for phosphate adsorption. In addition, results from elemental, SEM–EDS, and XRD analyses revealed that the DSTC surface was covered with colloidal or nano-sized MgO (periclase) particles, which could serve as the main adsorption sites for phosphate removal [27].

SEM–EDS analysis of the post-adsorption DSTC samples confirmed the hypothesis that the MgO particles on the DSTC surface may dominate the phosphate adsorption. At a high resolution of 7000×, when the SEM was focused on the MgO crystals on the P-loaded DSTC surface, the corresponding EDS spectrum of the SEM image focusing area showed an elevated peak of phosphorus (Fig. 1). Although phosphorus was also detected in the original DSTC, its EDS signal of phosphorus was much lower [27]. For the P-loaded DSTC, the phosphorus signal was even higher than those of the magnesium and oxygen, which showed the second and third highest EDS peaks (Fig. 1).

Metal oxides have showed strong ability to adsorb negative charged compounds, such as phosphate and arsenate [29]. When in contact with water, the metal oxide surface becomes hydroxylated and thus introduces either a positive or negative surface charge, depending on the solution pH. The charge development of MgO on the biochar surface can be described in a simplified manner as [30]:

$$S_{MgO} - OH_2^+ \Leftrightarrow S_{MgO} - OH \Leftrightarrow S_{MgO} - O^- \quad (1)$$

where S_{MgO} denotes the MgO surface. The point of zero charge (PZC) of MgO is very high (PZC_{MgO} = 12 [31]), thus its surface is expected to be positively charged in most natural aqueous conditions. In aqueous solution, phosphate exists in four species with pK_a values of 2.12 (pK_{a1}), 7.21(pK_{a2}), and 12.67 (pK_{a3}). When solution pH is lower than PZC_{MgO}, the hydroxylated MgO surface can electrostatically attract negatively charged phosphate species to form mono-, and polynuclear complexes [30,32]:

$$S_{MgO} - OH_2^+ + H_2PO_4^- \Leftrightarrow S_{MgO}H_2PO_4 + H_2O,$$
$$\text{mononuclear } (0.12 < \text{pH} < 9.21) \quad (2.1)$$

$$2S_{MgO} - OH_2{}^+ + HPO_4^{2-} \Leftrightarrow (S_{MgO})_2HPO_4 + 2H_2O,$$
$$\text{binuclear } (5.21 < \text{pH} < 10.67) \quad (2.2)$$

$$3S_{MgO} - OH_2^+ + PO_4^{3-} \Leftrightarrow (S_{MgO})_3PO_4 + 3H_2O,$$
$$\text{trinuclear } (10.67 < \text{pH} < 12) \quad (2.3)$$

Although most of the initial solution pH values in this study were around 7, the reductions of aqueous phosphate during the experiments would affect the dynamics of solution pH [15,32]. This would increase the heterogeneity of the adsorption processes of phosphate onto the biochar to trigger both mono- and polynuclear interactions (i.e., Eqs. (2.1)–(2.3)).

3.2. Other potential adsorption mechanisms

Element analysis indicated that there were large amount of calcium in both DSTC (9.78%) and STC (4.41%), which is a biochar derived from undigested sugar beet tailings [27]. If the calcium was released from the biochars into the solution as free ions, they may remove phosphate through precipitation. However, preliminary assessment of STC showed almost no ability to remove aqueous phosphate [27]. In addition, the XRD spectra of the original and P-loaded DSTC were almost identical and showed no evidence of calcium-phosphate precipitates in the P-loaded biochar (Fig. 2a), suggesting that the precipitation might not be an important mechanism for phosphate removal. This could be explained by two reasons: (1) some of the calcium in the biochar was in form of calcite (Fig. 2a), which has a very low solubility; and (2) a portion of the calcium might be incorporated inside of the biochar and could not be released into the solution [33].

Because there was abundance of surface functional groups on the DSTC surface, phosphate could also be removed by the biochar through interacting with the functional groups. However, again, the similarity between the FTIR spectra of the original and P-loaded DSTC provides no evidence of adsorption of phosphate onto the surface functional groups in the P-loaded biochar (Fig. 2b).

3.3. Adsorption kinetics

The adsorption of phosphate onto the DSTC increased smoothly over time and reached equilibrium after 24 h (Fig. 3a). The slow kinetics further suggests that precipitation might not play an import role in the removal of phosphate by the biochar. Mathematical models were used to simulate the experimental kinetics. In addition to the commonly used pseudo-first-order and pseudo-second-order models, the Ritchie *N*_th-order model and Elevich

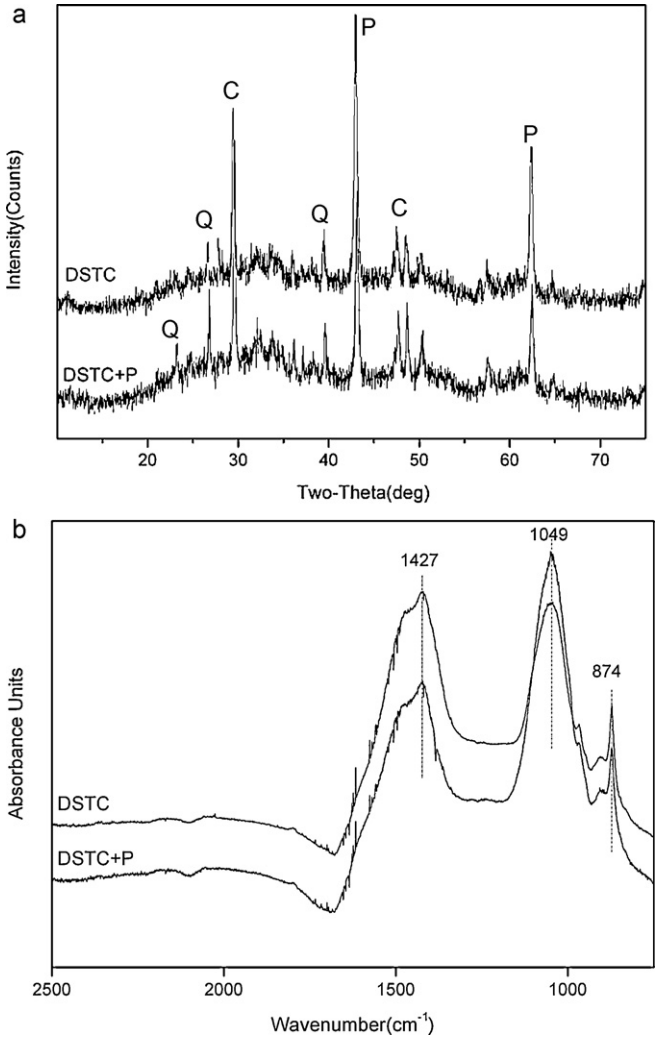

Fig. 2. XRD (a) and FTIR (b) spectra of the original and post-adsorption DSTC. Crystallites were detected with peaks labeled in the XRD spectra as Q for quartz (SiO_2), C for calcite ($CaCO_3$), and P for periclase (MgO).

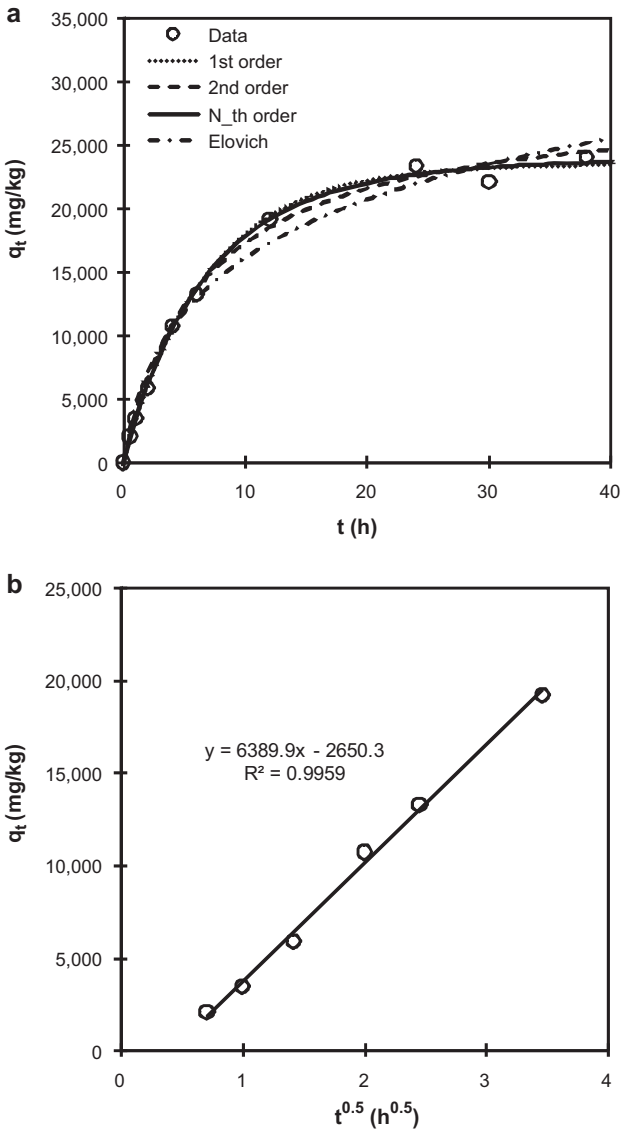

Fig. 3. Adsorption kinetic data and modeling for phosphate onto DSTC (a) full and (b) pre-equilibrium adsorption versus square root of time.

model were also tested [34] and are represented by the following equations:

$$\frac{dq_t}{dt} = k_1(q_e - q_t), \quad \text{first-order} \tag{3.1}$$

$$\frac{dq_t}{dt} = k_2(q_e - q_t)^2, \quad \text{second-order} \tag{3.2}$$

$$\frac{dq_t}{dt} = k_n(q_e - q_t)^N \quad N\text{\_th-order} \tag{3.3}$$

$$\frac{dq_t}{dt} = \alpha \exp(-\beta q_t), \quad \text{Elevich} \tag{3.4}$$

where q_t and q_e are the amount of phosphate adsorbed at time t and at equilibrium, respectively (mg kg^{-1}), and k_1, k_2 and k_n are the first-order, second-order, and N_th-order apparent adsorption rate constants (h^{-1}, kg mg^{-1} h^{-1}, and kg^N mg^{-N} h^{-1}), respectively. Also, α is the initial adsorption rate (mg kg^{-1}) and β is the desorption constant (kg mg^{-1}). The first-order, second-order, and N_th-order models describe the kinetics of the solid-solution system based on mononuclear, binuclear, and N-nuclear adsorption, respectively, with respect to the sorbent capacity [34], while the Elevich model is an empirical equation considering the contribution of desorption.

All the models closely reproduced the kinetic data (Fig. 3a), with all correlation coefficients (R^2) exceeding 0.98 (Table 1). However, the first-order, second-order, and N_th-order (N = 1.14) models fitted the data slightly better than the Elevich model and N_th-order model had the highest R^2 (0.997). This result is consistent with the proposed predominant mechanism that phosphate removal by the biochar was mainly through adsorption onto the colloidal and nano-sized MgO crystals on DSTC surface. Both mononuclear and polynuclear adsorption of phosphate would be favored in the kinetics experiment, perhaps explaining why fittings from the N_th-order model were slightly better than that of either the first- or second-order model.

Previous studies on the kinetic behaviors of microporous sorbents showed that intraparticle surface diffusion may be important to the adsorption process [35,36]. In this study, the adsorption of phosphate onto DSTC also showed diffusion limitation. The pre-equilibrium (i.e., before 24 h) phosphate adsorption showed a strong linear dependency (R^2 = 0.9959) on the square root of time (Fig. 3b). This result suggests that intraparticle surface diffusion may play an important role in controlling the adsorption of phosphate onto the biochar, likely due to its abundance of mesopores.

Table 1
Best-fit parameter values for models of kinetic and isotherm data.

Model	Parameter 1	Parameter 2	Parameter 3	R^2
First-order	$k_1 = 1.554 \times 10^{-1}$ h^{-1}	q_e = 23,475 mg kg^{-1}	–	0.9968
Second-order	$k_2 = 5.211 \times 10^{-6}$ kg mg^{-1} h^{-1}	q_e = 28,771 mg kg^{-1}	–	0.9949
*N*_th-order	$k_n = 7.008 \times 10^{-4}$ kg^N mg^{-N} h^{-1}	q_e = 23,928 mg kg^{-1}	N = 1.136	0.9970
Elevich	$\beta = 1.386 \times 10^{-4}$ mg kg^{-1}	α = 5968 mg kg^{-1}	–	0.9855
Langmuir	$K = 2.551 \times 10^{-2}$ L mg^{-1}	Q = 133,085 mg kg^{-1}	–	0.9526
Freundlich	$K_f = 1.164 \times 10^4$ mg$^{(1-n)}$ L^n kg^{-1}	n = 0.4527	–	0.9781
Langmuir–Freundlich	$K = 1.562 \times 10^{-2}$ L^n mg^{-n}	Q = 705,876 mg kg^{-1}	n = 0.4954	0.9785

3.4. Adsorption isotherms

With the maximum observed phosphate adsorption of greater than 100,000 mg kg^{-1} (Fig. 4), the DSTC showed phosphate sorption ability to be superior to most of the reported values of other carbonaceous adsorbents [2,15,16]. Three isotherm equations were tested to simulate the phosphate adsorption onto the biochar [34]:

$$q_e = \frac{KQC_e}{1 + KC_e}, \quad \text{Langmuir} \tag{4.1}$$

$$q_e = K_f C_e^n, \quad \text{Freundlich} \tag{4.2}$$

$$q_e = \frac{KQC_e^n}{1 + KC_e{}^n} \quad \text{Langmuir–Freundlich} \tag{4.3}$$

where K and K_f represent the Langmuir bonding term related to interaction energies (L mg^{-1}) and the Freundlich affinity coefficient (mg$^{(1-n)}$ L^n kg^{-1}), respectively, Q denotes the Langmuir maximum capacity (mg kg^{-1}), C_e is the equilibrium solution concentration (mg L^{-1}) of the sorbate, and n is the Freundlich linearity constant. The Langmuir model assumes monolayer adsorption onto a homogeneous surface with no interactions between the adsorbed molecules. The Freundlich and Langmuir–Freundlich models, however, are empirical equations, which are often used to describe chemisorptions onto heterogeneous surface.

All the models reproduced the isotherm data fairly well (Fig. 4), with correlation coefficients (R^2) exceeding 0.95 (Table 1). The Langmuir maximum capacity of DSTC was around 133,085 mg kg^{-1}, which is higher than that of many other adsorbents for the removal of phosphate from aqueous solutions (Table 2). Fittings of the Freundlich and Langmuir–Freundlich matched the experimental data better than those of the Langmuir model, suggesting the adsorption of phosphate onto the DSTC was controlled by heterogeneous processes. This result is consistent with the proposed predominant adsorption mechanism of phosphate removal by the biochar through both mononuclear and polynuclear adsorption onto the colloidal and nano-sized MgO particles on DSTC surface.

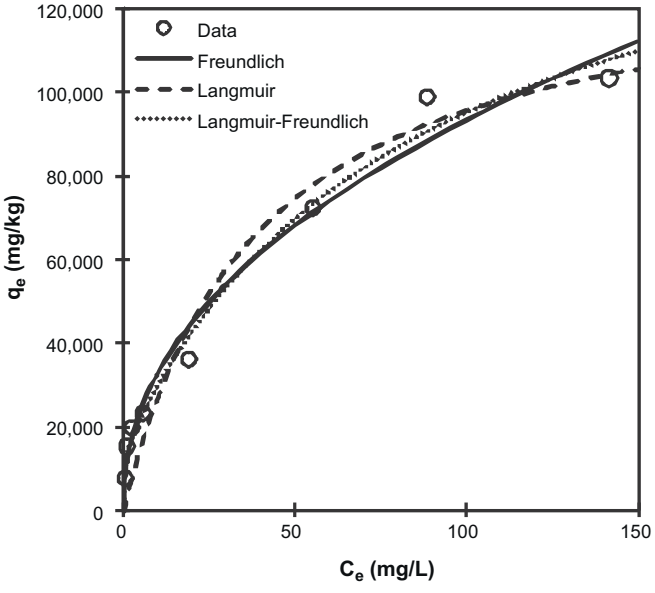

Fig. 4. Adsorption isotherm for phosphate on DSTC.

3.5. Effect of pH and coexisting anions

The adsorption of phosphate onto the DSTC depended on initial solution pH (Fig. 5a). The phosphate adsorption was lowest when pH equaled 2.0. When pH was increased from 2.0 to 4.1, the adsorption of phosphate by the biochar increased. Further increases in pH from 4.1 to 6.2, 7.1, 8.1, and 10.4, however, decreased the adsorption of phosphate onto the DSTC (Fig. 5a), suggesting the existence of an optimum pH for the maximum phosphate adsorption. This result is consistent with the proposed predominant adsorption mechanism that the optimum pH for phosphate removal by the colloidal and nano-sized MgO on biochar surface should be around 5.2, at which almost all phosphate exists in the form of $H_2PO_4^-$ (i.e., mononuclear adsorption). If solution pH is higher than the optimum value, polynuclear interactions may be triggered to consume more adsorption sites. Similar results were found in studies of the pH effect on phosphate removal from aqueous solution by other carbon-based adsorbents [15].

Although molecular concentrations of the coexisting anions were about 15.5 times of the phosphate, chloride and nitrate had little effect on the adsorption of phosphate (4.3 and 11.7 percent decrease, respectively) onto the biochar (Fig. 5b), suggesting low competitions between phosphate and these two ions for the MgO sites on the DSTC surface. The existence of high concentrations of bicarbonate in the solution, however, reduced the phosphate adsorption for about 41.4% (Fig. 5b). Two factors could be responsible for the reduction: (1) the competition for the adsorption site between bicarbonate and phosphate and (2) the increase of solution pH due to the addition of bicarbonate.

Table 2
Summary of the Langmuir maximum capacity of phosphate removal by different adsorbents.

Adsorbent	Q (mg kg^{-1})	Reference
Activated coir-pith carbon	5100–7262	[15,16]
Hydroxy-aluminum, hydroxy-iron, and hydroxy-iron–aluminum pillared bentonites	10,500–12,700	[37]
Functionalized nanoporous sorbent (FE-EDA-SAMMS)	43,300	[38]
Iron impregnated coir pith	70,920	[39]
Alunite	118,000	[2]
La(III)-, Ce(III)-, and Fe(III)-loaded orange waste	42,700	[40]
Metal loaded skin split waste	21,650–72,000	[41]
Slag and treated slag	32,900–60,700	[19]
Magnetic orange peel biochars	219–1240	[26]
DSTC	133,085	This work

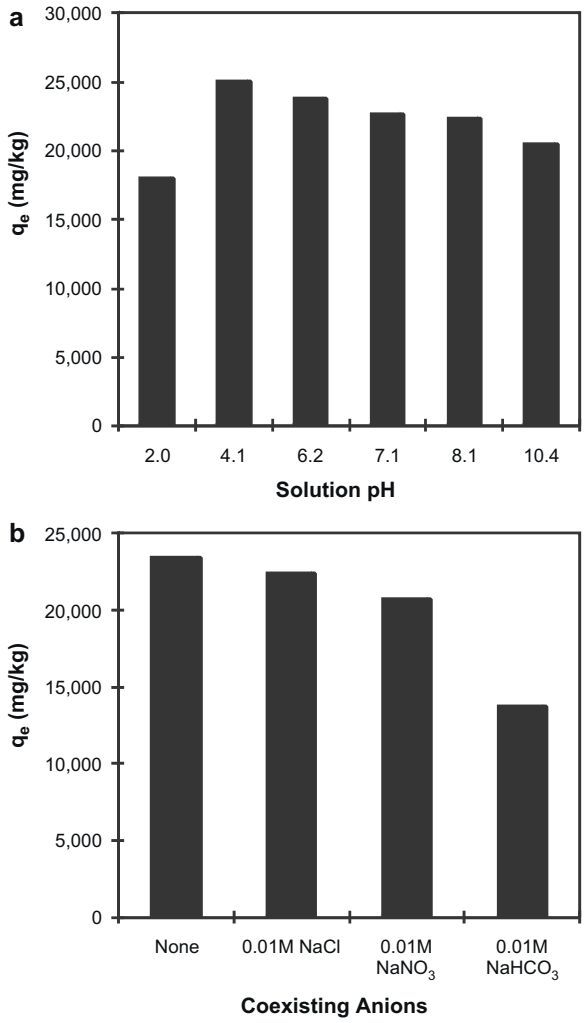

Fig. 5. Effect of (a) pH and (b) coexisting anions on phosphate adsorption onto DSTC.

4. Conclusions

Biochar converted from anaerobically digested sugar beet tailings (DSTC) demonstrated superior ability to remove phosphate from water under a range of pH and competitive ion conditions. Batch sorption experiments and post-sorption characterizations suggested that phosphate removal was mainly controlled by adsorption onto colloidal and nano-sized MgO particles on the DSTC surface. Because both the original and anaerobically digested sugar beet tailings are waste materials, the cost to make DSTC should be very low. However, the use of pre-digested sugar beet tailings has the benefit of additional energy generation and more efficient production (with less CO_2 release during production). Thus, DSTC should be considered a promising alternative water treatment or environmental remediation technology for phosphate removal. In addition, when used as an adsorbent to reclaim phosphate from water, the exhausted biochar can be directly applied to agricultural fields as a fertilizer to improve soil fertility because the P-loaded biochar contains abundance of valuable nutrients. Potential additional environmental benefits from this approach include fuel or energy produced during both the anaerobic digestion and pyrolysis and carbon sequestration due to biochar's refractory nature. Because arsenate and molybdate are phosphate analogues [29], it is expected that the digested sugar beet tailing biochar would also be an effective adsorbent for them.

Acknowledgements

This research was partially supported by the USDA T-STAR program and the NSF through grant CBET-1054405. The authors gratefully acknowledge Dr. Willie Harris for his assistance with the XRD analysis. The authors also thank the anonymous reviewers for providing input that led to improvement of the manuscript.

References

[1] D.S. Bhargava, S.B. Sheldarkar, Use of Tnsac in phosphate adsorption studies and relationships—literature, experimental methodology, justification and effects of process variables, Water Res. 27 (1993) 303–312.
[2] M. Ozacar, Adsorption of phosphate from aqueous solution onto alunite, Chemosphere 51 (2003) 321–327.
[3] S. Karaca, A. Gurses, M. Ejder, M. Acikyildiz, Kinetic modeling of liquid-phase adsorption of phosphate on dolomite, J. Colloids Interface Sci. 277 (2004) 257–263.
[4] C.P. Huang, Removal of phosphate by powdered aluminum-oxide adsorption, J. Water Pollut. Control Fed. 49 (1977) 1811–1817.
[5] S. Yeoman, T. Stephenson, J.N. Lester, R. Perry, The removal of phosphorus during waste-water treatment—a review, Environ. Pollut. 49 (1988) 183–233.
[6] D. Patureau, E. Helloin, E. Rustrian, T. Bouchez, J.P. Delgenes, R. Moletta, Combined phosphate and nitrogen removal in a sequencing batch reactor using the aerobic denitrifier, *Microvirgula aerodenitrificans*, Water Res. 35 (2001) 189–197.
[7] A. Gieseke, P. Arnz, R. Amann, A. Schramm, Simultaneous P and N removal in a sequencing batch biofilm reactor: insights from reactor- and microscale investigations, Water Res. 36 (2002) 501–509.
[8] L.E. de-Bashan, Y. Bashan, Recent advances in removing phosphorus from wastewater and its future use as fertilizer (1997–2003), Water Res. 38 (2004) 4222–4246.
[9] H.S. Altundogan, F. Tumen, Removal of phosphates from aqueous solutions by using bauxite. I. Effect of pH on the adsorption of various phosphates, J. Chem. Technol. Biotechnol. 77 (2002) 77–85.
[10] M. Singh, R.K. Srivastava, Sequencing batch reactor technology for biological wastewater treatment: a review, Asia-Pac. J. Chem. Eng. (2011) 3–13.
[11] T. Clark, T. Stephenson, A. Pearce, Phosphorus removal by chemical precipitation in a biological aerated filter, Water Res. 31 (1997) 2557–2563.
[12] R.D. Neufeld, G. Thodos, Removal of orthophosphates from aqueous solutions with activated alumina, Environ. Sci. Technol. 3 (1969) 661–667.
[13] G.A. Momberg, R.A. Oellermann, The removal of phosphate by hydroxyapatite and struvite crystallization in South-Africa, Water Sci. Technol. 26 (1992) 987–996.
[14] B.K. Biswas, K. Inoue, K.N. Ghimire, H. Harada, K. Ohto, H. Kawakita, Removal and recovery of phosphorus from water by means of adsorption onto orange waste gel loaded with zirconium, Bioresour. Technol. 99 (2008) 8685–8690.
[15] P. Kumar, S. Sudha, S. Chand, V.C. Srivastava, Phosphate removal from aqueous solution using coir-pith activated carbon, Sep. Sci. Technol. 45 (2010) 1463–1470.
[16] C. Namasivayam, D. Sangeetha, Equilibrium and kinetic studies of adsorption of phosphate onto $ZnCl_2$ activated coir pith carbon, J. Colloids Interface Sci. 280 (2004) 359–365.
[17] H. Yamada, M. Kayama, K. Saito, M. Hara, A fundamental research on phosphate removal by using slag, Water Res. 20 (1986) 547–557.
[18] N.M. Agyei, C.A. Strydom, J.H. Potgieter, An investigation of phosphate ion adsorption from aqueous solution by fly ash and slag, Cement Concrete Res. 30 (2000) 823–826.
[19] Y.J. Xue, H.B. Hou, S.J. Zhu, Characteristics and mechanisms of phosphate adsorption onto basic oxygen furnace slag, J. Hazard Mater. 162 (2009) 973–980.
[20] S. Karaca, A. Gurses, M. Ejder, M. Acikyildiz, Adsorptive removal of phosphate from aqueous solutions using raw and calcinated dolomite, J. Hazard Mater. 128 (2006) 273–279.
[21] G.N. Kasozi, A.R. Zimmerman, P. Nkedi-Kizza, B. Gao, Catechol and humic acid sorption onto a range of laboratory-produced black carbons (Biochars), Environ. Sci. Technol. 44 (2010) 6189–6195.
[22] X.D. Cao, L.N. Ma, B. Gao, W. Harris, Dairy-manure derived biochar effectively sorbs lead and atrazine, Environ. Sci. Technol. 43 (2009) 3285–3291.
[23] M. Uchimiya, I.M. Lima, K.T. Klasson, S.C. Chang, L.H. Wartelle, J.E. Rodgers, Immobilization of heavy metal ions (Cu-II, Cd-II, Ni-II, and Pb-II) by broiler litter-derived biochars in water and soil, J. Agric. Food Chem. 58 (2010) 5538–5544.
[24] Y Chun, G.Y. Sheng, C.T. Chiou, B.S. Xing, Compositions and sorptive properties of crop residue-derived chars, Environ. Sci. Technol. 38 (2004) 4649–4655.
[25] B.L. Chen, D.D. Zhou, L.Z. Zhu, Transitional adsorption and partition of nonpolar and polar aromatic contaminants by biochars of pine needles with different pyrolytic temperatures, Environ. Sci. Technol. 42 (2008) 5137–5143.
[26] B.L. Chen, Z.M. Chen, S.F. Lv, A novel magnetic biochar efficiently sorbs organic pollutants and phosphate, Bioresour. Technol. 102 (2011) 716–723.
[27] Y. Yao, B. Gao, M. Inyang, A.R. Zimmerman, X. Cao, P. Pullammanappallil, L. Yang, Biochar derived from anaerobically digested sugar beet tailings: Char-

acterization and phosphate removal potential, Bioresour. Technol. (2011), doi:10.1016/j.biortech.2011.1003.1006.
[28] USEPA, ESS Method 310.1: Ortho-phosphorus, Dissolved Automated, Ascorbic Acid, Environmental Sciences Section Inorganic Chemistry Unit, Wisconsin State Lab of Hygiene, 1992.
[29] B.A. Manning, S. Goldberg, Modeling competitive adsorption of arsenate with phosphate and molybdate on oxide minerals, Soil Sci. Soc. Am. J. 60 (1996) 121–131.
[30] P.W. Schindler, W. Stumm, The surface chemistry of oxides, hydroxides, and oxide minerals, in: W. Stumm (Ed.), Aquatic Surface Chemistry—Chemical Processes at the Particle–Water Interface, John Wiley & Sons, New York, 1987.
[31] M. Kosmulski, Surface Charging and Points of Zero Charge, Taylor & Francis Group, Boca Raton, FL, 2009.
[32] E.W. Shin, J.S. Han, M. Jang, S.H. Min, J.K. Park, R.M. Rowell, Phosphate adsorption on aluminum-impregnated mesoporous silicates: surface structure and behavior of adsorbents, Environ. Sci. Technol. 38 (2004) 912–917.
[33] X.D. Cao, W. Harris, Properties of dairy-manure-derived biochar pertinent to its potential use in remediation, Bioresour. Technol. 101 (2010) 5222–5228.
[34] C. Gerente, V.K.C. Lee, P. Le Cloirec, G. McKay, Application of chitosan for the removal of metals from wastewaters by adsorption—mechanisms and models review, Crit. Rev. Environ. Sci. Technol. 37 (2007) 41–127.
[35] R. Weerasooriya, H.J. Tobschall, W. Seneviratne, A. Bandara, Transition state kinetics of Hg(II) adsorption at gibbsite–water interface, J. Hazard. Mater. 147 (2007) 971–978.
[36] L. Axe, P. Trivedi, Intraparticle surface diffusion of metal contaminants and their attenuation in microporous amorphous Al, Fe, and Mn oxides, J. Colloids Interface Sci. 247 (2002) 259–265.
[37] L.G Yan, Y.Y. Xu, H.Q. Yu, X.D. Xin, Q. Wei, B. Du, Adsorption of phosphate from aqueous solution by hydroxy-aluminum, hydroxy-iron and hydroxy-iron–aluminum pillared bentonites, J. Hazard. Mater. 179 (2010) 244–250.
[38] W. Chouyyok, R.J. Wiacek, K. Pattamakomsan, T. Sangvanich, R.M. Grudzien, G.E. Fryxell, W. Yantasee, Phosphate removal by anion binding on functionalized nanoporous sorbents, Environ. Sci. Technol. 44 (2010) 3073–3078.
[39] K.A. Krishnan, A. Haridas, Removal of phosphate from aqueous solutions and sewage using natural and surface modified coir pith, J. Hazard. Mater. 152 (2008) 527–535.
[40] B.K. Biswas, K. Inoue, K.N. Ghimire, S. Ohta, H. Harada, K. Ohto, H. Kawakita, The adsorption of phosphate from an aquatic environment using metal-loaded orange waste, J. Colloids Interface Sci. 312 (2007) 214–223.
[41] X. Huang, X.P. Liao, B. Shi, Adsorption removal of phosphate in industrial wastewater by using metal-loaded skin split waste, J. Hazard. Mater. 166 (2009) 1261–1265.